Geophysical Research Letters

RESEARCH LETTER
10.1029/2021GL096783

New Insights on the Radiative Impacts of Ozone-Depleting Substances

Gabriel Chiodo[1,2] **and Lorenzo M. Polvani**[2,3]

[1]Institute for Atmospheric and Climate Science, ETH Zurich, Switzerland, [2]Department of Applied Physics and Applied Mathematics, Columbia University, New York, NY, USA, [3]Lamont-Doherty Earth Observatory, Columbia University, Palisades, NY, USA

Key Points:

- The radiative effect of Ozone-depleting substances on lower stratospheric temperatures is the largest of all well-mixed greenhouse gases
- Their radiative forcing is only partially (∼25%) canceled by the stratospheric ozone depletion they induce
- Their radiative forcing is weaker at the pole than at the equator opposing Arctic amplification even more than CO_2 forcing

Supporting Information:

Supporting Information may be found in the online version of this article.

Correspondence to:

G. Chiodo,
gabriel.chiodo@env.ethz.ch

Citation:

Chiodo, G., & Polvani, L. M. (2022). New insights on the radiative impacts of ozone-depleting substances. *Geophysical Research Letters*, *49*, e2021GL096783. https://doi.org/10.1029/2021GL096783

Received 28 OCT 2021
Accepted 6 MAY 2022

Author Contributions:

Conceptualization: Gabriel Chiodo, Lorenzo M. Polvani
Data curation: Gabriel Chiodo
Formal analysis: Gabriel Chiodo
Funding acquisition: Gabriel Chiodo, Lorenzo M. Polvani
Investigation: Gabriel Chiodo
Methodology: Gabriel Chiodo
Project Administration: Gabriel Chiodo, Lorenzo M. Polvani
Resources: Gabriel Chiodo, Lorenzo M. Polvani
Validation: Gabriel Chiodo
Visualization: Gabriel Chiodo
Writing – original draft: Gabriel Chiodo

Abstract The global warming potential of Ozone-depleting substances (ODS) has long been known to be thousands of times larger than the one of CO_2, but their climate impacts as greenhouse gases, i.e. unmediated ozone depletion, has received relatively little attention. Focusing on the period 1955–2005, we here present results from offline radiative forcing (RF) calculations from a global chemistry climate model. Using realistic distributions of ODS and consistent stratospheric ozone, we show that ODS dominate the adjusted stratospheric warming of the lower stratosphere, where CO_2 has little radiative impact. We also show that the global mean RF of stratospheric ozone only cancels a fraction of the RF of ODS, leaving an important ODS contribution to anthropogenic forcing. Finally we show that the RF of ODS opposes Arctic amplification, its equator-to-pole gradient being larger than the one of CO_2.

Plain Language Summary In the decades following World War II, organic compounds of chlorine and bromine, widely used in refrigerators and spray cans, entered the atmosphere and led to the formation of the ozone hole. However, these compounds, are also powerful greenhouse gases and are important for global warming. Here we study their warming effects in the stratosphere and at the surface. We find that, over the period 1955–2005, they were the dominant atmospheric gas warming the tropical lower stratosphere, where CO_2 is largely inactive; that their surface warming effect (their radiative forcing) amounted to approximately one third of the CO_2 value, even after accounting for reductions due to the ozone depletion they induce; and, finally that, even more than CO_2, their radiative effects warmed the equatorial more the polar regions and, as such, cannot be the reason why the Arctic is warming more than the rest of the planet.

1. Introduction

Anthropogenic emissions of chlorofluorocarbons (CFCs) and other chlorinated species have greatly enhanced stratospheric halogen abundance over the second half of the twentieth century (World Meteorological Organization, 2018), and thereby led to substantial depletion of the ozone layer. The widespread, though indirect, climatic impacts of ODS via ozone depletion, largely linked to the the shift of the Southern Hemispheric circulation, are well documented (Polvani et al., 2011; Previdi & Polvani, 2014; Thompson & Solomon, 2002). But ODS also impact the climate system in ways that are not mediated by ozone, since they are potent well-mixed greenhouse gases (Ramanathan, 1975). Recent studies have shown that the surface warming from ODS may have played a key-role in the observed weakening trends of the Walker circulation (Polvani & Bellomo, 2019), and in the warming of the Arctic and the associated sea ice loss (Polvani et al., 2020). These studies suggest that the direct climate impacts of ODS, as greenhouse gases, may deserve closer study. In this paper, as a first step, we seek a deeper understanding of the purely radiative effects of ODS.

Radiative forcing (RF) provides an important metric to evaluate and contrast the climatic impacts of different atmospheric trace gases (Ramaswamy et al., 2019). It is well established that ODS are powerful greenhouse gases (Ramanathan, 1975), with global warming potentials over a 100-year time horizon (GWP100) thousands of times larger than CO_2 (Hodnebrog, Aamaas, et al., 2020). However, the RF of ODS remains subject to some uncertainty. Detailed spectral calculations of the ODS RF using Line-by-Line (LbL) codes, routinely included in IPCC reports (e.g., Hodnebrog et al., 2013), typically employ two single (1-D) atmospheric profiles (tropical/extratropical) as this is the best compromise between computational expediency and accuracy (errors are less than 1% compared to calculations with better spatial resolution). Moreover, ODS in these models are typically assumed to be uniformly distributed, and assumptions concerning their lifetime are made to try to capture spatial

Writing – review & editing: Gabriel Chiodo, Lorenzo M. Polvani

inhomogeneities (Hodnebrog, Aamaas, et al., 2020). Lastly, LbL calculations only report the direct RF of ODS, without accounting for the accompanying ozone depletion, making these calculations somewhat unrepresentative of the actual forcing from ODS on the climate system.

Beyond LbL studies, the RF of ODS has also been quantified using radiative transfer schemes commonly included in global climate models. These have a coarser spectral resolution, but consider more realistic distributions of ODS, and also account for the indirect effects via ozone depletion. These studies have consistently shown that, over the second half of the twentieth century, the positive RF of ODS was offset by the negative RF of the stratospheric ozone losses they induce (Myhre et al., 2014, their Table 8.SM.6), but the degree of this cancellation remains highly uncertain (P. Forster et al., 2021, see Section 7.3.2.5). Two influential single-model studies using the stratosphere-adjusted RF have reported a very large cancellation, up to 80% (Ramaswamy et al., 1992; Shindell et al., 2013). In contrast, other studies based on model inter-comparison projects, have reported a much smaller cancellation, owing to a smaller negative RF from ozone depletion (typically in the range −0.03 to −0.1 W/m^2; Checa-Garcia et al., 2018; Cionni et al., 2011; Conley et al., 2013; Skeie et al., 2020). Unfortunately, the ozone fields used in some of these ODS RF estimates were taken from chemistry climate models (CCMs) different from the ones used to obtain the ODS distributions, yielding inconsistent net RF estimates.

In addition, two recent studies have suggested that the effective radiative forcing (ERF) from ODS, including adjustments beyond ozone depletion (e.g., tropospheric temperature and cloud changes), may be considerably smaller than previously thought. Using an emergent constraint approach based on CMIP6 models, Morgenstern et al. (2020) inferred an ERF of ODS between −0.05 and 0.13 W/m^2, concluding that the ODS-driven changes in stratospheric ozone and rapid adjustments effectively cancel the direct RF of ODS. This finding calls into question the conclusion of the IPCC-AR5 concerning the net RF of ODS being "very likely" positive. Another recent multi-model study using AerChemMIP models showed that ODS-driven ozone RF ranges between −0.05 and −0.3 W/m^2 (Thornhill et al., 2021). However, there is considerable uncertainty in these estimates. Taken together, the extent to which the RF from stratospheric ozone depletion cancels the RF from ODS RF remains unclear.

In addition to RF itself, the radiative adjustment of stratospheric temperatures to ODS forcing is also a matter of considerable interest. P. M. Forster and Joshi (2005) showed that ODS radiatively warm the tropical tropopause, but used an idealized model and assumed uniform ODS concentrations in the stratosphere. Another study, using a comprehensive CCM, revealed that the impacts of halocarbons (i.e., ODS and other, non-ozone-depleting, chlorine compounds) on the UTLS temperature are offset not only by changes in ozone, but also by water vapor changes and dynamical upwelling (McLandress et al., 2014). Those additional changes complicate our understanding of the purely radiative effect of ODS on temperature. Computing the radiative effects in isolation, as we do here, is a crucial first step in assessing the more complex dynamical, thermodynamical and chemical feedbacks associated with ODS.

Building on previous work, therefore, we here explore in detail the impact of ODS on stratospheric temperatures, as well as their RF, in a realistic and consistent setting, and and we place ODS in the context of the other Greenhouse-Gases (GHGs) and ozone. In particular, we address these questions: What is the structure of the radiative temperature adjustment caused by ODS in the stratosphere ? Does it depend on the spatial distribution of ODS? Does it depend on the local ODS concentrations or on their tropospheric abundances? How does it compare, quantitatively, to the one caused by the other GHGs and ozone? What is the net RF forcing of ODS, once the effects of stratospheric ozone depletion and stratospheric adjustments are considered? What is the latitudinal structure of the RF from ODS and does it contribute to Arctic Amplification? To answer these questions, we have run offline calculations with a CCM using the fixed dynamical heating approximation, following the technique pioneered by Fels et al. (1980). We find that ODS have the largest (warming) effect of all GHG on tropopause temperatures; that stratospheric ozone depletion cancel only a fraction of the RF of ODS; and, that the spatial pattern of the RF of ODS, even more than the one of CO_2, opposes Arctic amplification.

2. Methods

Input data for our offline radiative forcing calculations are taken from an ensemble of 6 historical simulations with the Whole Atmosphere Community Climate Model, version 4 (WACCM hereafter), previously analyzed in Polvani and Bellomo (2019); Polvani et al. (2020). These are transient atmosphere-ocean-land-sea-ice coupled model runs with interactive halocarbon and stratospheric ozone chemistry, covering the period 1955–2005, forced

with all known natural and anthropogenic forcings following the prescriptions of the Climate Model Intercomparison Project, phase 5 (CMIP5, Taylor et al., 2012). These simulations have been carefully validated: they show realistic climatology and trends, including the formation of the Antarctic ozone hole (see Marsh et al., 2013, for details). The modeled ozone trends over 1960–2000 are consistent with the observational SPARC data-set (not shown), and the vertical profiles of major CFC species (e.g., CFC12) are in excellent agreement with MIPAS (Eckert et al., 2016; Hoffmann et al., 2008). Also, inorganic chlorine (Cly) in WACCM closely matches observations, suggesting that the vertical fractional release in the model is realistic (see Eyring et al., 2010, for details). To estimate the RF, nearly instantaneous (i.e., hourly) three-dimensional distributions of ODS, ozone and other well-mixed GHGs from these simulations are averaged over our ensemble of 6 realizations to minimize the noise produced by internal variability (as in Kay et al., 2015).

These ensemble-averaged ODS concentrations are then used as input to the Parallel Offline Radiation Tool (PORT) of the Community Earth System Model (CESM; Conley et al., 2013). PORT isolates WACCM's radiative transfer module, and is configured with the same vertical and horizontal resolution. As in many other climate models (e.g., McLandress et al., 2014; Shine et al., 2003), only the radiative effects of CFC11 and CFC12 are computed explicitly in the WACCM/PORT radiation scheme. The effect of the other ODS is included by inflating CFC11 concentrations with a weighted sum, where the weights are the radiative efficiencies of each ODS relative to the efficiency of CFC11. This field, denoted CFC11*, is calculated as follows in WACCM/PORT:

$$\begin{aligned}\left[\mathrm{CFC11}^{*}\right] = [\mathrm{CFC11}] + \frac{0.30}{0.25}\cdot[\mathrm{CFC113}] + \frac{0.13}{0.25}\cdot[\mathrm{CCl_4}] + \frac{0.06}{0.25}\cdot[\mathrm{CH_3CCl_3}] \\ + \frac{0.20}{0.25}\cdot[\mathrm{HCFC22}] + \frac{0.30}{0.25}\cdot[\mathrm{CBrClF_2}] + \frac{0.32}{0.25}\cdot[\mathrm{CBrF_3}]\end{aligned} \quad (1)$$

where the brackets indicate the mixing ratios (in ppb) for each species, the numerators in the fractional coefficients indicate the radiative efficiency (in W/m^2/ppb) of each species, and the denominator the efficiency of CFC11 (0.25). Many more ODS than those in Equation 1 are included in WACCM's stratospheric chemistry module which are important for ozone chemistry, but only the ones above (The choice to only include the compounds in Equation 1 in the radiative scheme rests with the WACCM model develpment team (Marsh et al., 2013). We here simply follow their choice, since we need to make our PORT radiative calculations consistent with the historical CMIP5 WACCM simulations they performed. Nonetheless, we have estimated the RF of the minor ODS not included in Equation 1, using Table 4 of Hodnebrog, Aamaas, et al. (2020), and they only amount to less than 7% of the total halocarbon forcing) are used to compute the radiative fluxes. Lumping the effect of these ODS species into the CFC11* field is a reasonable approximation, given that the stratospheric temperature adjustment of each individual species is estimated to be almost identical (within a few %) of that of CFC12 and CFC11 (cf. Figure 4 of Hodnebrog, Aamaas, et al., 2020). As the WACCM version used here was set up for CMIP5, the efficiency values come from Table 2.14 of P. M. Forster et al. (2007). Recent updates (reported in Hodnebrog, Aamaas, et al., 2020) should not significantly alter the results, as they generally lie within 5% of the values in Equation 1. The largest revision is for CCl_4 (0.17 vs. our value of 0.13), but this species only makes up a modest (less than 5%) contribution to the total RF of ODS (Hodnebrog, Aamaas, et al., 2020).

We wish to emphasize that unlike RF calculations with LbL codes which seek to compute with maximum accuracy a single RF number, our priority here is to elucidate the spatial structure of the radiative impacts of ODS, consistently with ozone and other forcings, in the fully coupled historical simulations of our model, where important climate impacts due to ODS have been previously documented.

To be consistent with our WACCM historical simulations which were performed over the period 1955–2005, we focus on that same period here. This period was originally chosen because it captures the growth of ODS to their peak abundance (World Meteorological Organization, 2018). Since ODS emissions prior to 1955 are tiny (cumulative emissions were at 20 Gg/y, i.e., less than 5% of those registered by 2000, see e.g., McCulloch et al. (2003)), the RF calculated here should be close to those reported by the IPCC assessments (1750-present). Focusing on that period then, two steps are needed to calculate the radiative effects of ODS. First, we carry out a "baseline" PORT run with ensemble mean values for meteorological variables (e.g., temperature, clouds, etc), the spatial distribution of radiatively active species (CO_2, ODS, ozone, etc), and the zonal mean tropopause height specified from the average over the period 1955–1960 of the transient historical WACCM simulations. Second, we run a set of "perturbation" PORT runs, each time replacing a specific gas for which the RF needs to be calculated (e.g., ODS) with the concentrations of that gas obtained from averaging over the period 2000–2005 of the same

historical simulations. We use hourly instantaneous input meteorological and composition fields (averaged over 6 members), following the approach of Conley et al. (2013) to ensure accuracy in the calculations. To be clear: all the meteorological variables, including clouds and water vapor, are specified at the year 1955–1960, since changes in such quantities are part of the rapid adjustments and do not belong to the computation of the stratosphere-adjusted RF (see Summary and Discussion).

For each PORT run we compute the annual and global average tropopause-level shortwave and longwave fluxes, after stratospheric temperatures reach equilibrium: RF is then defined as the difference between the perturbed fluxes and the baseline fluxes. In addition, we diagnose the temperature correction needed to achieve radiative equilibrium within the stratosphere, denoted ΔT_{adj} and refereed to as the "stratospheric temperature adjustment" in the "fixed dynamical heating" approximation (Fels et al., 1980), ΔT_{adj} quantifies the radiative impact on stratospheric temperatures of the species considered. In order to contrast ODS to other forcings, we also compute RF and ΔT_{adj} over the same period for all other well-mixed GHGs (CO_2, CH_4 and N_2O), and for ozone (again, taken from the same WACCM runs for consistency).

3. Results

Before presenting our results for RF and ΔT_{adj} we illustrate the time evolution and the spatial distribution of ODS over the period of interest (1955–2005). The timeseries of globally averaged surface volume mixing ratios of CFC11* and CFC12, as prescribed in the WACCM historical simulations, are shown in Figures 1a and 1b, respectively. Both increase steadily between 1960 and 1990, but CFC12 plateaus thereafter, whereas CFC11* increases further as it includes HCFCs which are still increasing (Hodnebrog, Aamaas, et al., 2020). Next, the latitude-height distributions of CFC11* and CFC12 in WACCM are shown in Figures 1c and 1d, respectively. The main sink of these compounds is photolysis in the stratosphere, so they are well-mixed in the troposphere but rapidly decay with altitude above the tropopause, with larger concentrations at low latitudes since the main stratospheric entry point is the tropical tropopause and the tracer is carried aloft via tropical upwelling. CFC12 decreases from 500 ppt near the tropopause (10–12 km) to about 100 ppt near 10 hPa (30 km), which is in excellent agreement with MIPAS (Hoffmann et al., 2008; see also Figure 4.6.1 of Hegglin & Tegtmeier, 2017). Good agreement with measurements is also found for the CFC11 vertical profiles (not shown). These figures suggest that the assumption of vertically uniform ODS profiles in the stratosphere, common to previous global modeling studies (P. M. Forster & Joshi, 2005; McLandress et al., 2014) is inaccurate in the stratosphere. The degree to which this affects RF calculations in our global climate model is discussed below.

We start by exploring the stratospheric temperature adjustment (ΔT_{adj}) due to ODS, shown in Figure 2a. As is well known, ODS cause a substantial warming of the global stratosphere (recall that tropospheric temperatures are kept fixed in these calculations), with peaks of 0.2–0.3 K in the subtropical lower stratosphere. Note that while stratospheric ODS concentrations peak in the deep tropics (Figures 1c and 1d), the largest warming is found in the subtropics. This is due to the radiative properties of ODS and the climatological atmospheric conditions. ODS have the strongest absorption bands at 9 and 11 μm, where the atmosphere is optically thin (Shine, 1991). At these wavelengths, in the stratosphere, the ODS absorption of upwelling radiation from the surface and troposphere exceeds the amount of radiation emitted by the ODS, due to the large temperature difference between the stratosphere and the source of the upwelling radiation, and this leads to a net warming. However, that warming is modulated by the amounts of atmospheric humidity and cloud coverage, which alter the effective emission temperature. As seen in Figure S1 of Supporting Information S1, the minimum in cloud fraction at the edge of the subtropical dry zones, together with smaller precipitable water than at the equator, leads to weaker masking and locally larger upwelling LW in the subtropical dry zones (20–30°N/S), and hence a maximum warming there, with weaker warming in the cloudier and moister deep tropics (10N-10S).

The warming pattern in our model is qualitatively similar to the one in P. M. Forster and Joshi (2005, see their Figure 2a), but with two key differences. First, ours is weaker by about 30%–40%. Second, our ΔT_{adj} reaches its maximum in the subtropics, not at the equator. These differences are likely due to several idealizations in their study: their use of (a) spatially uniform and larger CFC concentrations, (b) clear-sky atmospheric profiles, and (c) a lower and globally uniform tropopause (5 km). In fact, we find good spatial agreement with McLandress et al. (2014), although our ΔT_{adj} cannot be directly compared with theirs (as their Figure A1 shows the heating rate, in K/day, not ΔT_{adj}). Nonetheless, we conclude that the radiative warming of the tropical lower stratosphere

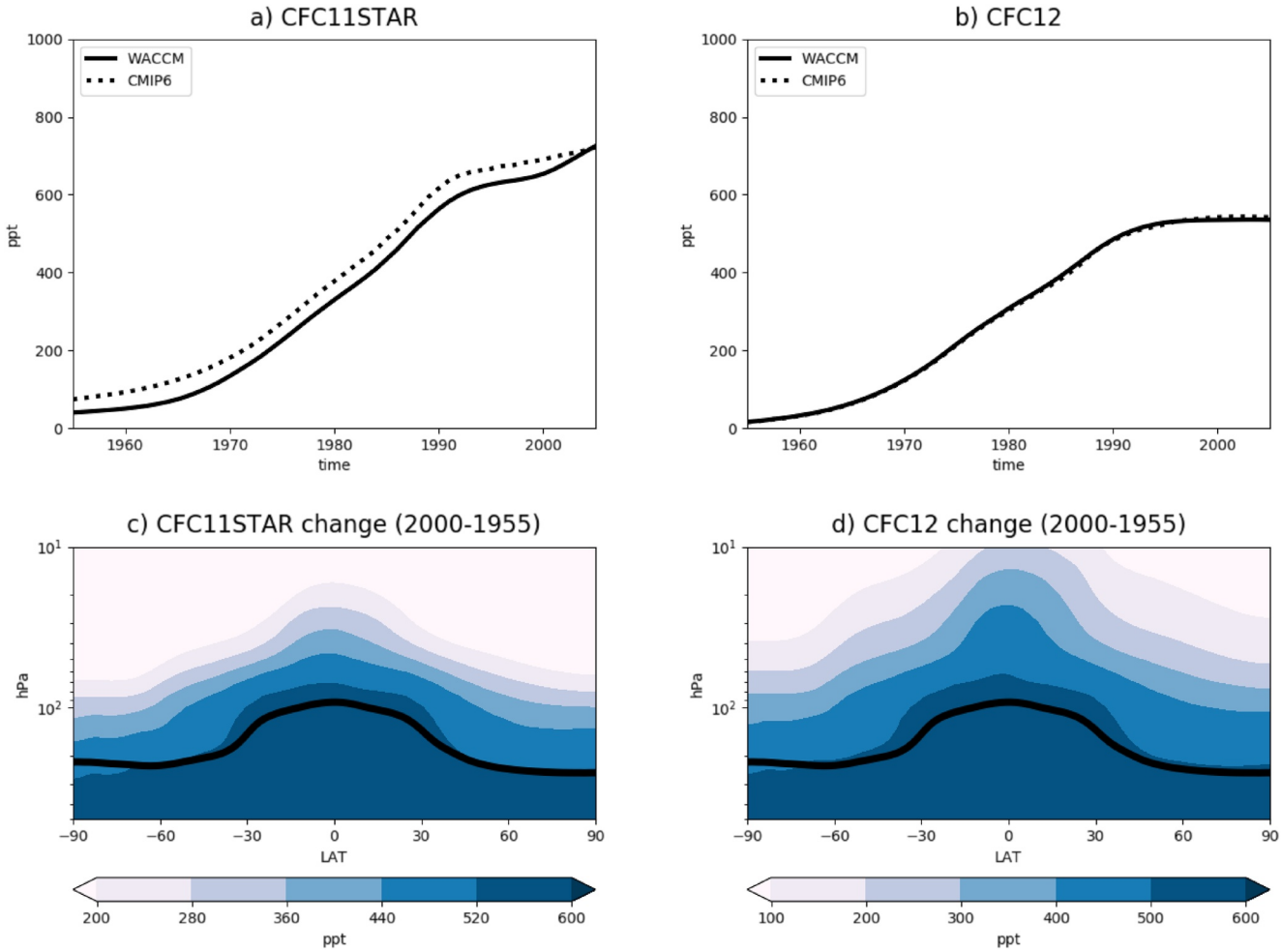

Figure 1. (a) Time evolution of the annual mean, global mean, surface volume mixing ratios of CFC11*, in ppt, specified at the lower boundary of the WACCM model between 1955 and 2005. (b) As in (a), but for CFC12. (c) Annual mean, zonal mean change over the period 2005-1955 in CFC11*, in ppt, with the black line showing the annual mean tropopause. (d) As in (c) but for CFC12.

by ODS, and the maximum off the equator, are robust features in agreement with previous studies and consistent with our understanding of the radiative properties of ODS.

One may now wonder whether the warming pattern in Figure 2a is primarily due to the well-mixed tropospheric or to the non-uniform stratospheric ODS concentrations. To answer this question, we performed two additional PORT runs, imposing the stratospheric and tropospheric ODS concentrations separately; the resulting ΔT_{adj} are shown in Figures 2c and 2d, respectively. These reveal that the stratospheric ODS are key to creating the stratospheric warming pattern (Figure 2c), whereas tropospheric ODS have little effect on ΔT_{adj} (Figure 2d). Hence the *local* absorption by ODS molecules exceeding the increased emissions creates the pattern. Also, the "filtering" of LW from the Earth's surface by tropospheric ODS is negligible, owing to their very low concentrations (in ppt, typically): this clearly justifies the "weak absorber" approximation (Shine & Myhre, 2020).

We now place the impact of ODS on stratospheric temperatures in the context of the other well-mixed GHGs. We do this by calculating ΔT_{adj} for CO_2, CH_4 and N_2O separately (shown in Figure S3 of Supporting Information S1), and then combining them with ODS to show the total temperature response from all well-mixed GHGs (Figure 2b). As expected, CO_2 cools the stratosphere, with a maximum in the upper stratosphere (see, e.g., Shine et al., 2003). This is due to an increase in local emission (cooling to space) accompanied by additional absorption of upwelling LW radiative flux from the lower atmospheric levels. As the upwelling LW radiative flux originating from the surface is almost entirely absorbed by CO_2 in the troposphere at 4.3 and 15 μm, the LW flux absorbed by stratospheric CO_2 originates from upper tropospheric (and thus colder) levels. Therefore, local

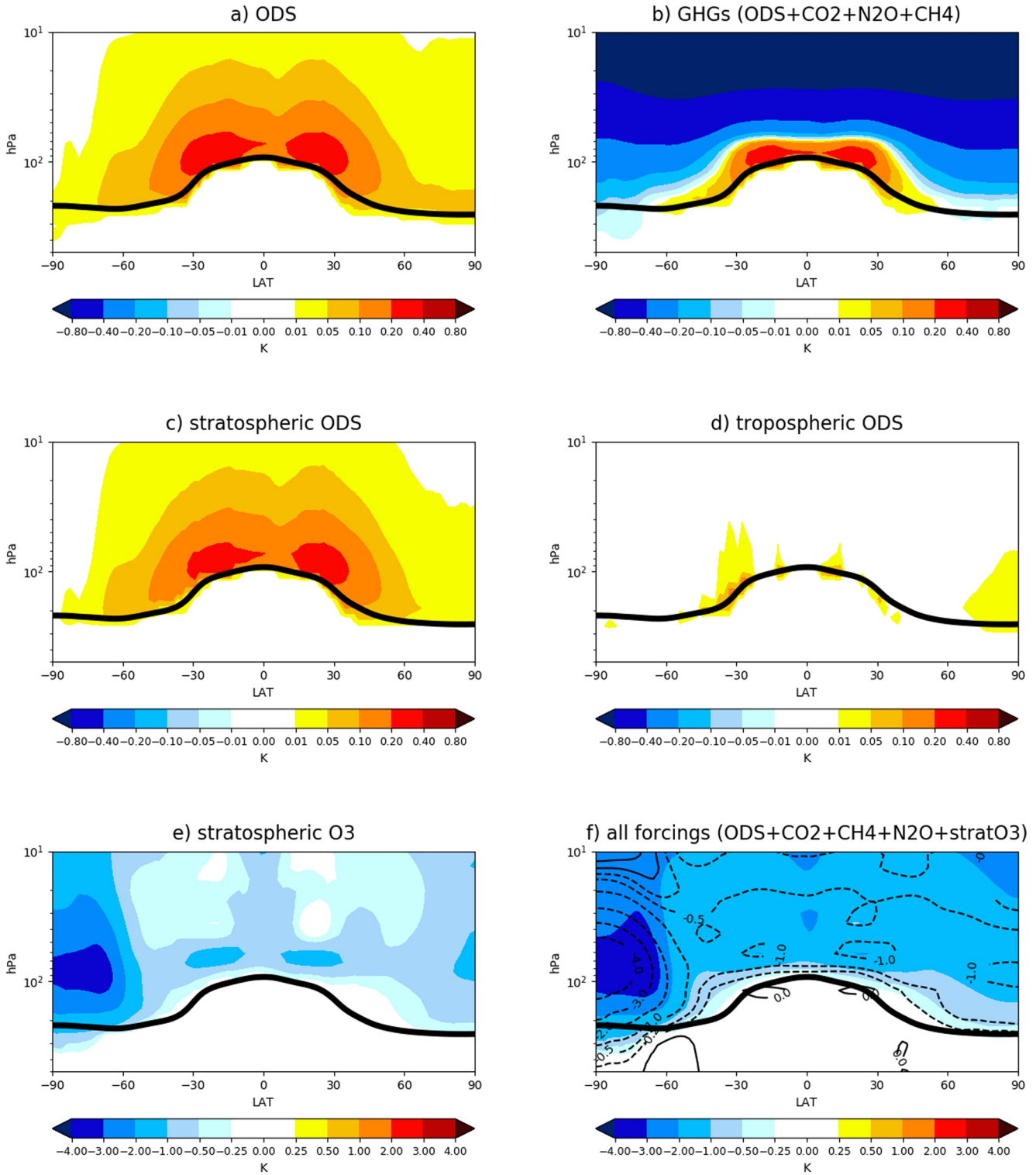

Figure 2. Annual mean, zonal mean stratospheric temperature adjustment (ΔT_{adj}), in K, induced by changes between 1955 and 2005 in (a) ODS, (b) all well-mixed GHGs (CO_2 + N_2O + CH_4 + ODS), (c) stratospheric ODS, (d) tropospheric ODS, (e) stratospheric ozone, and (f) all forcings together. The black dashed contours in (f) show the temperature change in free-running, fully coupled WACCM runs historical runs, computed as the difference between the 1995–2005 mean and the 1955–1965, averaged over an ensemble of 6 simulations. In all panels, the thick black line shows the tropopause.

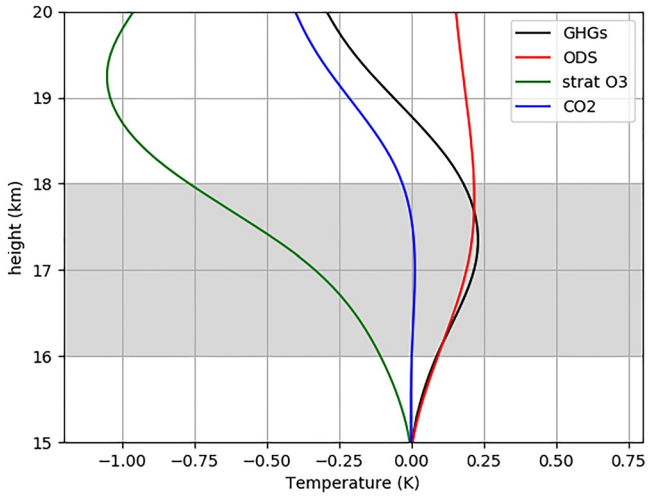

Figure 3. Tropical vertical profile (15N-15S mean) of the stratospheric temperature adjustment (ΔT_{adj}, in K) in the tropopause region. Different colors correspond to different forcings, as indicated in the legend. The gray shading highlights the cold point tropopause.

emission outweighs absorption, leading to cooling. This effect maximizes in the upper stratosphere, due to warm temperatures there and thus more efficient emission (Ramanathan, 1998). The remaining GHGs (CH_4 and N_2O) have a negligible effects on stratospheric temperatures (Figure S3b and S3c in Supporting Information S1), due to spectral overlap with water vapor and CO_2 absorption bands (Etminan et al., 2016). The key point we wish to convey with Figure 2b is that the radiative warming from ODS is much larger than the cooling from CO_2 in the lower stratosphere. As a consequence, the radiative temperature response to well-mixed GHGs is shaped by ODS in this region: between 100-70 hPa, ODS set up a latitudinal temperature gradient of almost 1 K, which is absent at higher levels where CO_2 dominates.

The role of ODS is especially crucial in the tropical lower stratosphere, a region whose temperature controls the amount of water vapor entering the stratosphere, with major implications for chemistry and climate. To highlight the importance of ODS in that region, we plot the vertical profile of ΔT_{adj} in Figure 3, averaged from 15°S to 15°N. Nearly all the radiative warming around the cold-point tropopause (around 16–18 km) is caused by ODS (contrast the red and black lines). More importantly, between 16 an 17 km the warming from ODS nearly cancels the cooling associated with stratospheric ozone depletion (green line), making ODS concentrations key to understanding multi-decadal trends in the UTLS (upper troposphere and lower stratosphere) region.

In nearly all other regions, however, the stratospheric cooling from ozone depletion is large, as shown in Figure 2e (note the color scale difference between panels b and e), and is especially prominent in the Southern polar stratosphere (with a peak of nearly 4 K there), consistent with the formation of the Antarctic ozone hole. For the sake of completeness, we conclude by showing the total ΔT_{adj} from GHG and stratospheric ozone combined in Figure 2f. In that panel, we have superimposed (in dashed black lines) the stratospheric temperature changes over the same period from the free-running historical WACCM simulations. The PORT calculations capture the main features of the temperature changes in WACCM and the differences, locally as large as 20%–30%, are due to changes in the stratospheric circulation. This becomes clear when examining the absolute temperature differences between PORT and WACCM (Figure S2 in Supporting Information S1) which reveals a dipole of warm/cool anomalies in the lower stratosphere, suggesting that dynamical warming/cooling contributes to a portion of observed temperature trends in WACCM. This indicates that historical stratospheric temperature changes are, to a good degree, radiatively driven, thus validating the FDH approximation.

While ozone depletion appears to largely obliterate stratospheric warming induced by ODS, except in the tropical lower stratosphere, we now show that it does not play a dominant role in the estimates of radiative forcing, to which we now turn our attention. Consider first the total RF due to all well-mixed GHGs combined (CO_2 + N_2O + CH_4 + ODS), whose latitudinal structure is shown in Figure 4a (solid black line): its global mean value is 1.48 W/m^2 in our PORT calculations. Of this, 0.32 W/m^2 are due to ODS (red line), in agreement (to within 7%) with the LbL estimated of Hodnebrog et al. (2013) and in even better agreement with updated RF values from IPCC-AR6 (P. Forster et al., 2021), based on Hodnebrog, Aamaas, et al. (2020, cf. their Table 4). With a 22% contribution to the total GHG forcing, ODS are thus the largest source of global warming after carbon dioxide over the period 1955–2005 in our model. In particular, the ODS contribution is larger than the one of tropospheric ozone (0.29 W/m^2), shown in Figure S4 of Supporting Information S1. The RF of ODS is also larger than methane (0.30 W/m^2), but it is possible that our model underestimates the shortwave absorption bands of CH_4(see e.g., Etminan et al., 2016). Factoring in a 15% upward correction in the methane RF, ODS would be the third most important GHG over 1955–2005.

But what about the depletion of stratospheric ozone that accompanies ODS increases? Three studies examined the question, and concluded that ozone depletion largely cancels the RF of ODS (Morgenstern et al., 2020; Ramaswamy et al., 1992; Shindell et al., 2013), thus making ODS a minor player for global warming. However, Ramaswamy et al. (1992) was based on a very short time period (1979–1990, barely one decade), and Shindell et al. (2013) was based on a single model with notable ozone biases (see their Figure 2). The third study

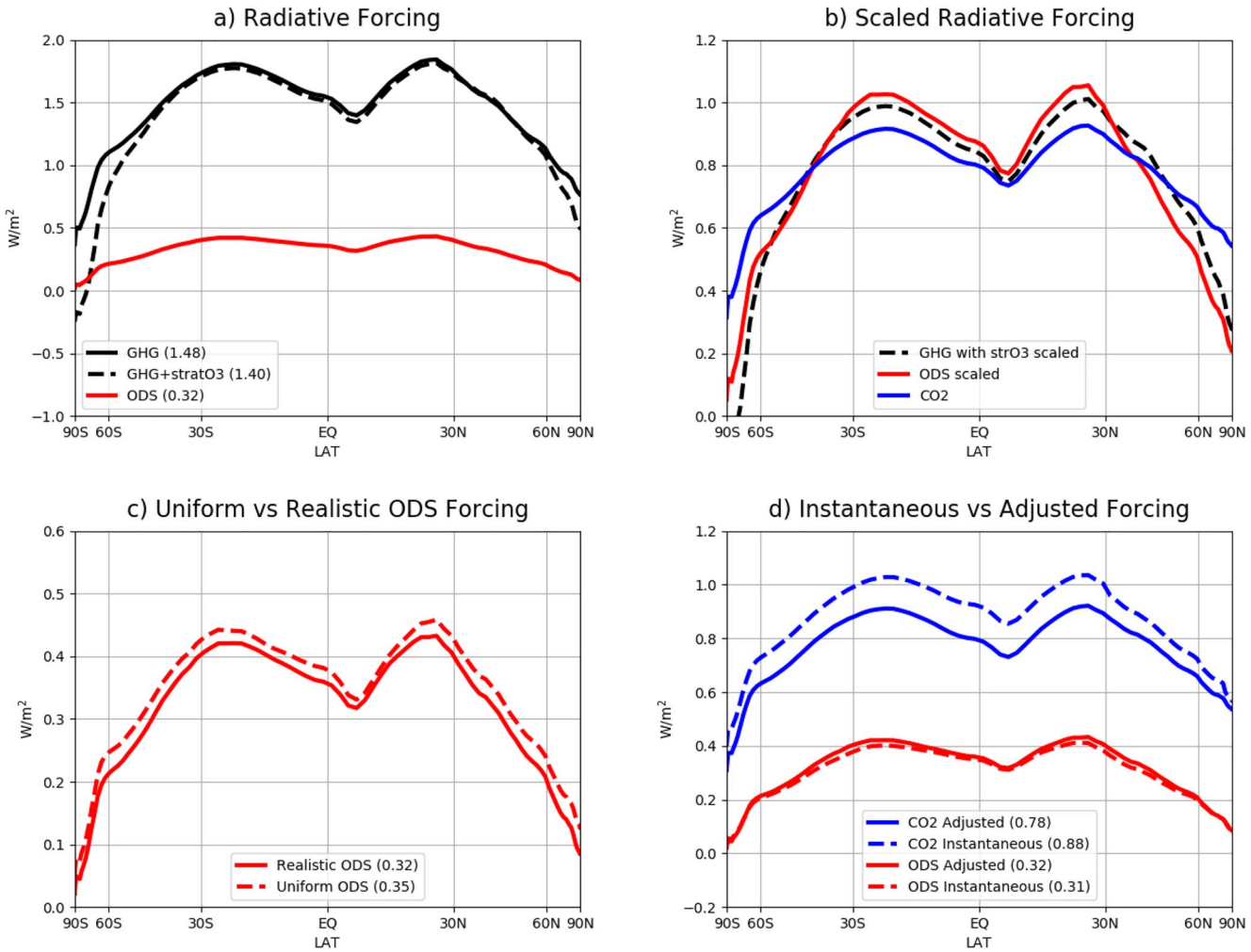

Figure 4. (a) Stratospherically adjusted radiative forcing, in W/m^2 over the period 1955–2005 for ODS alone (red), all well-mixed GHGs (CO_2 + N_2O + CH_4 + ODS, solid black), and GHGs plus stratospheric ozone (dashed black). (b) As in (a), but with GHG plus stratospheric ozone and ODS to match the global mean value of CO_2 (0.78 W/m^2, blue). (c) As in (a), but for realistic (solid) and uniform (dashed) ODS distributions. (d) As in (a) but for the instantaneous (dashed) and stratospherically adjusted (solid) forcing, for ODS (red) and CO_2 (blue).

(Morgenstern et al., 2020), focusing on ERF rather than RF, reported a large cancellation, but is based on two models (UKESM and CNRM) with an unrealistically strong depletion (Skeie et al., 2020). Also, the fact that the RF from ozone does not scale linearly with total column ozone (Lacis et al., 1990) is at odds with the emergent constraint approach of that study. Hence, for different reasons, the conclusion of a large cancellation reported in these studies is questionable.

Using WACCM/PORT we here reach the opposite conclusion, in agreement with several multi-model studies (Checa-Garcia et al., 2018; Cionni et al., 2011; Conley et al., 2013). As seen in Figure 4a (black dashed line) including stratospheric ozone depletion only reduces the total RF due to GHGs from 1.48 to 1.40 W/m^2, as ozone losses only substantially affect RF in the polar regions. This small RF of stratospheric ozone in WACCM/PORT is entirely consistent with the values reported multi-model means of the CMIP5 and CMIP6 models (see Table 1, column 8, rows 1–7 of Checa-Garcia et al., 2018). Our stratospheric ozone RF (−0.08 W/m^2) amounts to only a quarter of the ODS RF, so that the combined forcing of ODS and stratospheric ozone is still considerable (0.24 W/m^2) in our model.

Beyond the global mean value, it is important to explore the latitudinal structure of the RF of ODS, as it has been suggested that surface warming might be larger for forcing agents that are predominantly acting in the high latitudes (Shindell, 2014; Stuecker et al., 2018). This raises the possibility that large Arctic surface warming and sea

ice loss caused by ODS reported by Polvani et al. (2020), who analyzed the same WACCM historical simulations used here, could be related to the latitudinal structure of the ODS RF. However, as we see in Figure 4a, the RF latitudinal dependence for ODS is similar to the one for the well-mixed GHGs, with smaller values at the poles than at the equator. Hence, the RF of ODS opposes Arctic amplification.

We further explore the latitudinal structure of the ODS RF by asking: is the equator-to-pole RF gradient of ODS larger or smaller than of CO_2? To answer this, we scale each RF to match the global mean RF of CO_2 alone (0.78 W/m^2), and plot these scaled RFs in Figure 4b. Surprisingly, we find that the ODS curves are considerably steeper than the CO_2 curves: in other words, the RF of ODS opposes Arctic amplification even more than the RF of CO_2. And the addition of stratospheric ozone further increases the equator-to-pole gradient, by decreasing the net RF over the poles. Taken together, these results clearly indicate that ODS (and stratospheric ozone) would reduce polar amplification when added to CO_2, if radiative forcing were the dominant effect.

Finally, we explore the impact on RF of (a) using a non-uniform ODS distribution and (b) allowing for stratospheric adjustments (ΔT_{adj}): these have traditionally been either neglected or simplified in past IPCC assessment reports (P. M. Forster et al., 2007; Myhre et al., 2014), and were only recently factored in for complex LbL studies reported in the IPCC-AR6 (P. Forster et al., 2021). As shown in Figure 4c, when the same value for the tropospheric ODS as the one shown in Figures 1c and 1d is spread uniformly across the stratosphere, the resulting RF is found to be larger by 0.03 W/m^2: while this is relatively small, it nonetheless represents a 10% overestimate, and could be easily corrected. We add, however, that spreading ODS uniformly has very little effect on ΔT_{adj} in the lower stratosphere (not shown). As for the impact of stratospheric adjustment: as seen in Figure 4d, the inclusion of stratospheric temperature adjustment considerably decreases the RF of CO_2 by 12% (from 0.88 to 0.78 W/m^2), as reported previously (e.g., Shine & Myhre, 2020). In contrast, the stratospheric adjustment increases the RF of ODS by about 4% (from 0.31 to 0.32 W/m^2), primarily at low latitudes. These values are broadly similar albeit somewhat smaller than recent estimates (10%) from a more sophisticated narrow-band model (Shine & Myhre, 2020), where a more complete discussion of this interesting effect can be found. Including the stratospheric adjustment slightly increases the RF of ODS in the subtropical and mid-latitude regions (compare bold vs. stippled red lines in Figure 4d), thereby partly contributing to the large equator-to-pole gradient in the RF of ODS (Figure 4b).

4. Summary and Discussion

The aim of this paper has been to explore the radiative effects of ODS, notably the temperature change they produce in the stratosphere and their radiative forcing, including its latitudinal structure, and to situate ODS in the context of other well mixed greenhouse gases and of stratospheric ozone. We have been especially careful to accomplish this in a consistent manner, using realistic ODS distributions from the same chemistry-climate model from which the ozone was computed interactively, and computing RF with the same offline radiative transfer code as the one in the climate model itself. Also, rather than the typical 1750 (or 1850) to present period, we have focused on the historical period 1955–2005, over which ODS went from near zero to a maximum.

Three key results have emerged from our study. First, we have shown that ODS cause a considerable radiative warming in the tropical lower stratosphere and, in that region (where CO_2 plays no significant radiative role), the warming from ODS nearly cancels the cooling caused by ozone depletion. Hence, ODS are of major importance for understanding tropical lower stratospheric temperature trends, and the associated impact on water vapor entering the stratosphere.

Second, we have shown that stratospheric ozone depletion only cancels a fraction of the RF from ODS (25% in our model), in agreement with recent studies (e.g., Checa-Garcia et al., 2018). As a result of this cancellation, the net RF of ODS including the indirect effects from stratospheric ozone in our climate model is 0.24 W/m^2, which amounts to nearly one third of the radiative forcing of CO_2 over the period 1955–2005. Note that a net positive RF of ODS is also consistent with the IPCC-AR6, which suggests a RF of 0.02 W/m^2 (P. Forster et al., 2021) from stratospheric ozone trends over 1850–2019 (Section 7.3.2.5), and an ODS (emission-driven) ozone RF of −0.15 W/m^2 (Thornhill et al., 2021): these values are smaller than the direct RF of ODS (0.32 W/m^2), further supporting the results obtained with our climate model.

Third, we have shown that the latitudinal structure of the RF caused by ODS, while broadly similar to those of other GHGs (larger at the equator than at the poles), has an even steeper latitudinal gradient than the RF of CO_2, thus opposing Arctic Amplification even more strongly. This offers important new evidence that the large Arctic impact of ODS reported in an earlier study (Polvani et al., 2020), which analyzed the same historical simulations, must be due to strong local feedbacks, notably changes in the lapse rate feedback reported in Liang et al. (2022).

We acknowledge that calculating a purely radiative forcing, as we have done here, has recently fallen into disfavor, as so-called "fast-adjustments" (i.e., forced changes that precede any surface temperature changes) need to be incorporated as part of the forcing of the climate system, not as part of its response to a forcing agent. To accomplish this, the CMIP6 recommends computing an effective radiative forcing (ERF), obtained by running a model with the forcing agent added but with fixed sea surface temperature, as explained in P. M. Forster et al. (2016). But this may not be needed for ODS: analyzing model output from the Precipitation Driver Response Model Intercomparison Project (Myhre et al., 2017), a recent study has shown that ERF is fairly similar to RF in the case of ODS (Hodnebrog, Myhre, et al., 2020). Additional fast adjustments due to changes in methane lifetime or cloud-circulation changes associated with ozone have been explored by Thornhill et al. (2021), who found them to be small or strongly model dependent (e.g., clouds). Therefore, we have good reason to believe that the key results presented here would not be fundamentally altered if such additional rapid adjustments were included.

Data Availability Statement

The data analyzed in this study is available for access to the community on Zenodo at http://zenodo.org/record/6413013#YktqoyRBwUE.

Acknowledgments
The work of L.M.P. is supported by the US National Science Foundation under award 1914569. G.C. was supported by the SNSF Ambizione award PZ00P2_180043. We greatly acknowledge Michael Kiefer, Andrea Linden and Gabriele Stiller (KIT) for providing CFC data for validation of the WACCM model. We also acknowledge D.Kinnison and two anonymous reviewers for their useful comments. Open access funding provided by Eidgenossische Technische Hochschule Zurich.

References

Checa-Garcia, R., Hegglin, M. I., Kinnison, D., Plummer, D. A., & Shine, K. P. (2018). Historical tropospheric and stratospheric ozone radiative forcing using the cmip6 database. *Geophysical Research Letters*, *45*(7), 3264–3273.

Cionni, I., Eyring, V., Lamarque, J.-F., Randel, W., Stevenson, D., Wu, F., et al. (2011). Ozone database in support of CMIP5 simulations: Results and corresponding radiative forcing. *Atmospheric Chemistry and Physics*, *11*(21), 11267–11292. https://doi.org/10.5194/acp-11-11267-2011

Conley, A., Lamarque, J.-F., Vitt, F., Collins, W., & Kiehl, J. (2013). PORT, a CESM tool for the diagnosis of radiative forcing. *Geoscientific Model Development*, *6*(2), 469–476. https://doi.org/10.5194/gmd-6-469-2013

Eckert, E., Laeng, A., Lossow, S., Kellmann, S., Stiller, G., Von Clarmann, T., et al. (2016). Mipas imk/iaa cfc-11 (ccl 3 f) and cfc-12 (ccl 2 f 2) measurements: Accuracy, precision and long-term stability. *Atmospheric Measurement Techniques*, *9*(7), 3355–3389. https://doi.org/10.5194/amt-9-3355-2016

Etminan, M., Myhre, G., Highwood, E., & Shine, K. (2016). Radiative forcing of carbon dioxide, methane, and nitrous oxide: A significant revision of the methane radiative forcing. *Geophysical Research Letters*, *43*(24), 12–614. https://doi.org/10.1002/2016gl071930

Eyring, V., Shepherd, T., & Waugh, D. (2010). *Sparc report on the evaluation of chemistry-climate models*.

Fels, S., Mahlman, J., Schwarzkopf, M., & Sinclair, R. (1980). Stratospheric Sensitivity to Perturbations in Ozone and Carbon Dioxide: Radiative and Dynamical Response. *Journal of the Atmospheric Sciences*, *37*(10), 2265–2297. https://doi.org/10.1175/1520-0469(1980)037<2265:sstpio>2.0.co;2

Forster, P., Storelvmo, T., Armour, K., Collins, W., Dufresne, J.-L., Frame, D., et al. (2021). The earth's energy budget, climate feedbacks, and climate sensitivity. In *Climate change 2021 - the physical science basis: Working group i contribution to the sixth assessment report of the intergovernmental panel on climate change*. Cambridge University Press.

Forster, P. M., & Joshi, J. (2005). The role of halocarbons in the climate change of the troposphere and stratosphere. *Climatic Change*, *71*(1–2), 249–266. https://doi.org/10.1007/s10584-005-5955-7

Forster, P. M., Ramaswamy, V., Artaxo, P., Berntsen, T., Betts, R., Fahey, D., et al. (2007). Changes in atmospheric constituents and in radiative forcing. In *Climate Change 2007: The Physical Science Basis. Contribution of Working Group I to the Fourth Assessment Report of the Intergovernmental Panel on Climate Change*. Cambridge University Press.

Forster, P. M., Richardson, T., Maycock, A. C., Smith, C. J., Samset, B. H., Myhre, G., et al. (2016). Recommendations for diagnosing effective radiative forcing from climate models for CMIP6. *Journal of Geophysical Research: Atmospheres*, *121*(20), 12–460. https://doi.org/10.1002/2016jd025320

Hegglin, M. I., & Tegtmeier, S. (2017). *The sparc data initiative: Assessment of stratospheric trace gas and aerosol climatologies from satellite limb sounders (Tech. Rep.)*. ETH Zurich.

Hodnebrog, O., Aamaas, B., Fuglestvedt, J., Marston, G., Myhre, G., Nielsen, C., et al. (2020). Updated global warming potentials and radiative efficiencies of halocarbons and other weak atmospheric absorbers. *Reviews of Geophysics*, *58*(3), e2019RG000691. https://doi.org/10.1029/2019rg000691

Hodnebrog, O., Etminan, M., Fuglestvedt, J., Marston, G., Myhre, G., Nielsen, C., et al. (2013). Global warming potentials and radiative efficiencies of halocarbons and related compounds: A comprehensive review. *Reviews of Geophysics*, *51*(2), 300–378. https://doi.org/10.1002/rog.20013

Hodnebrog, O., Myhre, G., Kramer, R. J., Shine, K. P., Andrews, T., Faluvegi, G., et al. (2020). The effect of rapid adjustments to halocarbons and N2O on radiative forcing. *npj Climate and Atmospheric Science*, *3*(1), 1–7. https://doi.org/10.1038/s41612-020-00150-x

Hoffmann, L., Kaufmann, M., Spang, R., Müller, R., Remedios, J. J., Moore, D., et al. (2008). Envisat mipas measurements of cfc-11: Retrieval, validation, and climatology. *Atmospheric Chemistry and Physics*, *8*(13), 3671–3688. https://doi.org/10.5194/acp-8-3671-2008

Kay, J. E., Deser, C., Phillips, A., Mai, A., Hannay, C., Strand, G., et al. (2015). The Community Earth System Model (CESM) Large Ensemble Project. *Bulletin of the American Meteorological Society*, *96*(8), 1333–1349. https://doi.org/10.1175/bams-d-13-00255.1

Lacis, A. A., Wuebbles, D. J., & Logan, J. A. (1990). Radiative forcing of climate by changes in the vertical distribution of ozone. *Journal of Geophysical Research: Atmospheres*, *95*(D7), 9971–9981. https://doi.org/10.1029/jd095id07p09971

Liang, Y.-C., Polvani, L. M., Previdi, M., Smith, K. L., England, M. R., & Chiodo, G. (2022). Stronger arctic amplification from ozone-depleting substances than from carbon dioxide. *Environmental Research Letters*, *17*(2), 024010. https://doi.org/10.1088/1748-9326/ac4a31

Marsh, D. R., Mills, M. J., Kinnison, D. E., Lamarque, J.-F., Calvo, N., & Polvani, L. M. (2013). Climate change from 1850 to 2005 simulated in CESM1 (WACCM). *Journal of Climate*, *26*(19), 7372–7391. https://doi.org/10.1175/jcli-d-12-00558.1

McCulloch, A., Midgley, P. M., & Ashford, P. (2003). Releases of refrigerant gases (cfc-12, hcfc-22 and hfc-134a) to the atmosphere. *Atmospheric Environment*, *37*(7), 889–902. https://doi.org/10.1016/s1352-2310(02)00975-5

McLandress, C., Shepherd, T. G., Reader, M. C., Plummer, D. A., & Shine, K. P. (2014). The climate impact of past changes in halocarbons and CO2 in the tropical UTLS region. *Journal of Climate*, *27*(23), 8646–8660. https://doi.org/10.1175/jcli-d-14-00232.1

Morgenstern, O., O'Connor, F. M., Johnson, B. T., Zeng, G., Mulcahy, J. P., Williams, J., et al. (2020). Reappraisal of the climate impacts of ozone-depleting substances. *Geophysical Research Letters*, *47*(20), e2020GL088295. https://doi.org/10.1029/2020gl088295

Myhre, G., Forster, P., Samset, B., Hodnebrog, O., Sillmann, J., Aalbergsjø, S., et al. (2017). Pdrmip: A precipitation driver and response model intercomparison project—Protocol and preliminary results. *Bulletin of the American Meteorological Society*, *98*(6), 1185–1198. https://doi.org/10.1175/bams-d-16-0019.1

Myhre, G., Shindell, D., & Pongratz, J. (2014). Anthropogenic and natural radiative forcing supplementary material. In *Climate Change 2013 - The Physical Science Basis: Working Group I Contribution to the Fifth Assessment Report of the Intergovernmental Panel on Climate Change* (pp. 659–740). Cambridge University Press. https://doi.org/10.1017/CBO9781107415324.018

Polvani, L. M., & Bellomo, K. (2019). The Key Role of Ozone-Depleting Substances in weakening the Walker Circulation in the Second Half of the Twentieth Century. *Journal of Climate*, *32*(5), 1411–1418. https://doi.org/10.1175/jcli-d-17-0906.1

Polvani, L. M., Previdi, M., & Deser, C. (2011). Large cancellation, due to ozone recovery, of future Southern Hemisphere atmospheric circulation trends. *Geophysical Research Letters*, *38*(4). https://doi.org/10.1029/2011gl046712

Polvani, L. M., Previdi, M., England, M. R., Chiodo, G., & Smith, K. L. (2020). Substantial twentieth-century Arctic warming caused by ozone-depleting substances. *Nature Climate Change*, *10*(2), 130–133. https://doi.org/10.1038/s41558-019-0677-4

Previdi, M., & Polvani, L. M. (2014). Climate system response to stratospheric ozone depletion and recovery. *Quarterly Journal of the Royal Meteorological Society*, *140*(685), 2401–2419. https://doi.org/10.1002/qj.2330

Ramanathan, V. (1975). Greenhouse effect due to chlorofluorocarbons: Climatic implications. *Science*, *190*, 50–52. https://doi.org/10.1126/science.190.4209.50

Ramanathan, V. (1998). Trace-gas greenhouse effect and global warming: *Underlying principles and outstanding issues volvo environmental prize lecture-1997* (pp. 187–197). Ambio.

Ramaswamy, V., Collins, W., Haywood, J., Lean, J., Mahowald, N., Myhre, G., et al. (2019). Radiative forcing of climate: The historical evolution of the radiative forcing concept, the forcing agents and their quantification, and applications. *Meteorological Monographs*, *59*, 14–1. https://doi.org/10.1175/amsmonographs-d-19-0001.1

Ramaswamy, V., Schwarzkopf, M., & Shine, K. (1992). Radiative forcing of climate from halocarbon-induced global stratospheric ozone loss. *Nature*, *355*(6363), 810–812. https://doi.org/10.1038/355810a0

Shindell, D. (2014). Inhomogeneous forcing and transient climate sensitivity. *Nature Climate Change*, *4*(4), 274–277. https://doi.org/10.1038/nclimate2136

Shindell, D., Faluvegi, G., Nazarenko, L., Bowman, K., Lamarque, J.-F., Voulgarakis, A., et al. (2013). Attribution of historical ozone forcing to anthropogenic emissions. *Nature Climate Change*, *3*(6), 567–570. https://doi.org/10.1038/nclimate1835

Shine, K. P. (1991). On the cause of the relative greenhouse strength of gases such as the halocarbons. *Journal of the Atmospheric Sciences*, *48*(12), 1513–1518. https://doi.org/10.1175/1520-0469(1991)048<1513:otcotr>2.0.co;2

Shine, K. P., Bourqui, M., Forster, P. d. F., Hare, S., Langematz, U., Braesicke, P., et al. (2003). A comparison of model-simulated trends in stratospheric temperatures. *Quarterly Journal of the Royal Meteorological Society*, *129*(590), 1565–1588. https://doi.org/10.1256/qj.02.186

Shine, K. P., & Myhre, G. (2020). The spectral nature of stratospheric temperature adjustment and its application to halocarbon radiative forcing. *Journal of Advances in Modeling Earth Systems*, *12*(3), e2019MS001951. https://doi.org/10.1029/2019ms001951

Skeie, R. B., Myhre, G., Hodnebrog, Ø., Cameron-Smith, P. J., Deushi, M., Hegglin, M. I., et al. (2020). Historical total ozone radiative forcing derived from CMIP6 simulations. *npj Climate and Atmospheric Science*, *3*(1), 1–10. https://doi.org/10.1038/s41612-020-00131-0

Stuecker, M. F., Bitz, C. M., Armour, K. C., Proistosescu, C., Kang, S. M., Xie, S.-P., et al. (2018). Polar amplification dominated by local forcing and feedbacks. *Nature Climate Change*, *8*(12), 1076–1081. https://doi.org/10.1038/s41558-018-0339-y.…

Taylor, K., Stouffer, R., & Meehl, G. (2012). An overview of CMIP5 and the experiment design. *Bull. Am. Meterol. Soc.*, *93*, 485–498. https://doi.org/10.1175/bams-d-11-00094.1

Thompson, D. W., & Solomon, S. (2002). Interpretation of recent Southern Hemisphere climate change. *Science*, *296*(5569), 895–899. https://doi.org/10.1126/science.1069270

Thornhill, G. D., Collins, W. J., Kramer, R. J., Olivié, D., Skeie, R. B., O'Connor, F. M., et al. (2021). Effective radiative forcing from emissions of reactive gases and aerosols–a multi-model comparison. *Atmospheric Chemistry and Physics*, *21*(2), 853–874. https://doi.org/10.5194/acp-21-853-2021

World Meteorological Organization. (2018). *Executive Summary: Scientific Assessment of Ozone Depletion: 2018* (p. 67).